Electrochimica Acta 385 (2021) 138191

Contents lists available at ScienceDirect

Electrochimica Acta

journal homepage: www.elsevier.com/locate/electacta

Determination of the corrosion product layer resistance on zinc and electrolytically galvanized steel samples by using gel electrolytes

Svenja Valet*, Andreas Burkert, Gino Ebell, Martin Babutzka

Bundesanstalt für Materialforschung und –prüfung (BAM), Division 7.6 Corrosion and Corrosion Protection, Unter den Eichen 87, 12205 Berlin, Germany

ARTICLE INFO

Article history:
Received 15 December 2020
Revised 12 February 2021
Accepted 16 March 2021
Available online 1 May 2021

Keywords:
A: Gel electrolytes
A: agar
A: zinc coatings
C: atmospheric exposure
C: corrosion

ABSTRACT

Although zinc and zinc coatings have been widely used for corrosion protection for decades new zinc coatings are constantly being developed. Characterizing the corrosion protectiveness of these new coatings, however, should not be underestimated. While exposure tests are time intensive, cyclic tests can only be used for a very limited field of application. Thus, electrochemical measurements provide both an efficient and an effective alternative. Conventional aqueous bulk electrolytes influence the surface layers of a tested zinc coating and are therefore not reliable. Gel electrolytes, however, have evolved over the last few years, are minimally invasive and provide reliable results.

This work describes experiments with gel electrolytes made of agar. Unlike previous work, it proposes a composition of gel electrolyte for minimally invasive description of the protective power of naturally formed oxide layers on zinc and zinc coatings. Therefore, as a first part, the gel electrolyte made of agar is verified as a method for zinc and zinc-coated samples. Afterwards, this paper introduces the corrosion product layer resistance R_L as a promising parameter to evaluate the protective power of zinc coatings. Results are verified with EIS and FTIR measurements. An example on a representative zinc coating demonstrates the practical application.

1. Introduction

Besides iron, aluminium and copper, zinc belongs to one of the four most utilized metals in the world, not only as construction material, but also in biomedical applications and for physiology [1,2]. Its main use, however, is as a protective layer on steel and iron against corrosion. In 2017, the US reported that 87% of the total US consumption of zinc (517,000 t) was used for galvanizing processes [1].

Numerous publications exist about the atmospheric corrosion of zinc and zinc coatings (e.g. [2–9]). To predict the zinc corrosion rate under different atmospheric conditions world-wide exposure programs were performed during the last decades, e. g. the ISO-CORRAG [10] and the MICAT [11,12] program. Zinc forms spontaneously an oxide film of a few nm thickness, which converts into different corrosion products, depending on the type of atmosphere [2–5].

Due to the technical significance of zinc as corrosion protection, new zinc alloy coatings are being constantly developed [2,13], which in turn results in the formation of new corrosion products such as layered double hydroxide structures [14]. Assessing the corrosion resistance of these new coatings requires year-long field exposure tests. In order to minimize the time for analysing the corrosion behaviour, accelerated corrosion tests are widely used, such as the neutral salt spray test [7,15–18]. Due to a lack of resemblance of the atmospheric corrosion mechanisms, particularly the influence of wet-dry-cycles to zinc, which largely depend on the climatology [14,19], however, the results cannot be transferred onto natural field exposure results. Some standards and info sheets [20–23] already imply the non-reliability of cyclic tests. Consequently, while atmospheric exposure tests take too long time, and cyclic teste are unsuitable, electrochemistry seems to be a promising alternative.

Bulk electrolytes (that means a mass of electrolyte) used for electrochemical investigations may trigger the transformation or dissolution of formed corrosion products, hence being unsuitable for reactive oxide films and samples with corrosion products forming a kind of passivation layer. Furthermore, curved and irregular specimen surfaces may generate crevices in combination with mounted measuring cells [19,24]. The use of gel electrolytes prevents these problems, with the gel's impeded diffusion conditions preventing the dissolution of the corrosion prod-

* Corresponding author.
E-mail address: svenja.valet@bam.de (S. Valet).

https://doi.org/10.1016/j.electacta.2021.138191

uct layer [25]. Polymer electrolytes - ionically conducting material [26]- have been employed for more than 50 years [27,28], primarily for solid state electrochemical devices such as batteries or electrochromic devices [24,26,27,29]. While at the beginning polymer electrolytes were largely made of synthetic materials (such as poly(ethylene oxide)), natural polymers came into focus recently [26,30]. Besides being naturally abundant and thus renewable and biodegradable, they are inexpensive and easy to prepare [26,29,31]. Examples of such natural polymers are starch, cellulose, gelatine and agar [30]. Among them, agar is a promising material, as it is prone to a phenomenon called syneresis: the "spontaneous loss of water on standing" [32], which helps wetting the surface between the agar and of a sample surface with a thin moisture film, assuring an electrolytic electrode/sample contact [19,24,31].

Agar is a natural polysaccharide found in red seaweed. It is composed of agarose – the polysaccharide fraction with the greatest gelling potential – and agaropectin – the collective fraction of poor or non-gelling polysaccharides [32,33]. While both consist of the same backbone – agarobiose, a disaccharide –, agarose is neutral, but agaropectin is charged due to the partial replacement of side groups by pyruvic acid, sulphated or methylated groups, making it polar/hydrophobic [30,32,33]. Agar is commonly used in bacteriology or virology; however, it is also in use as gel electrolytes for electrochemistry [32,34].

Table 1 gives an overview of recent work on gel-type polymers which are made of agar and are used for corrosion testing. It can be seen that agar gels are mainly used for bronze, stainless steel and zinc. The compositions of the agar electrolyte, however, vary depending on the application. While previous research was based on the addition of salts or acids to achieve transparent gels with maximum conductivity for electrochromic devices [26,30,35] or to mimic bulk electrolytes [36,37], Table 1 focuses on agar gels used as electrolytes for investigating atmospheric corrosion phenomena. Previously, Angelini [38] studied the atmospheric corrosion on cultural heritage with disposable surface electrodes used for electrocardiograms. Although they found electrochemical impedance spectroscopy to be an effective method to study the formed corrosion layer, the conductivity of the electrodes is too low, and the inhomogeneous distribution of current may distort the findings. Therefore, the table at hand focuses on gel electrolytes made of agar.

Table 1 presents the differences in the composition of the various gel electrolytes used. Furthermore, it depicts the diverse electrochemical methods and analysed metal types.

Cano et al. [29] built a portable cell to be able to examine the natural patina of bronze sculptures. They demonstrated that the gelification of a liquid electrolyte with agar does not influence the results of the electrochemical impedance spectroscopy. However, the effect of agar on the results was not tested. Ramírez-Barat et al. [31] studied the effect of agar, showing that it slightly accelerates the anodic partial reaction, but does not influence the cathodic partial reaction on bronze samples. They were able to obtain reproducible results with electrochemical impedance spectroscopy without changing the corrosion mechanism. Ramírez-Barat et al. continued their work [41] and studied the influence of different reference electrodes and electrode distances, allowing for specific applications of their system.

Monrrabal et al. [24] used the knowledge gathered by Cano and Ramírez-Barat to modify the agar gel electrolyte by the addition of glycerol as a plasticizer. To simulate the aggressiveness of conventional aqueous electrolytes, sodium chloride was added. They proofed that the gel can successfully replace classical aqueous electrolytes for examining metallic surfaces. This was also found in other studies [36]. Monrrabal et al. continued their work [40] and added $KClO_4$ salts to their gel electrolytes in order to

Table 1
Overview of gel-electrolytes made of agar used for atmospheric corrosion investigations; scientific publications in peer-reviewed journals, sorted by year.

Author	Ingredients of gel electrolyte	Type of sample	Electrochemical method used	Year
Cano et al. [29]	5% (w/v) agar + 0.3 M NaCl in Milli-Q water	bronze coupons and sculpture	EIS	2014
Ramírez-Barat et al. [31]	1–5% (w/v) agar + 10 x concentrated artificial rain; adjusted to pH 6.5, $c(Cl^-) = 3.58^{-4}$ M	laminated and cast bronze coupons	EIS, polarization curves	2015
Monrrabal et al. [24]	0.5–2.5% (w/w) agar + 0–70% (w/w) glycerol + 0.5% (w/w) NaCl in distilled water	AISI 304 stainless steel	OCP, EIS, anodic polarization curves	2016
Babutzka et al. [25]	agar, $c(Cl^-) = 260$ ppm	pure zinc	polarization curves, electrochemical frequency modulation (EFM)	2017
Di Turo et al. [39]	5% (w/v) agar + 0.3 M NaCl in distilled water	bronze patina	EIS	2017
Monrrabal et al. [40]	0.5% (w/w) agar + 30–50% (w/w) glycerol + 0.5% NaCl or 1% $KClO_4$ salts (w/w) in distilled water	AISI 304 stainless steel sheet and tank	OCP, EIS, Mott Schottky	2018
Ramírez-Barat et al. [41]	3% agar (w/v) + 10 x concentrated artificial rain; adjusted to pH 6.5	laminated AISI 316 stainless steel, laminated and cast bronze coupons	EIS	2018
Monrrabal et al. [42]	0.5% (w/w) agar + 40% (w/w) glycerol + 0.5% (w/w) NaCl in distilled water	AISI 304 stainless steel	Electrochemical noise	2019
Langklotz et al. [19]	3% (w/v) agar in demineralized water, $c(Cl^-) = 60$ ppm	titanium zinc (99.5%)	EIS, OCP, linear polarization resistance, linear sweep voltammetry	2019

improve the electrolyte conductivity. They concluded that the selection of desired aggression is possible. Monrrabal et al., however, did not add the salt in their subsequent study with electrochemical noise to detect localized corrosion of stainless steel [42]. Instead, they used the optimized composition of their previous study [24].

In the meantime, Di Turo et al. [39] used the same gel electrolyte recipe as Cano et al. [29] for the study of ancient bronze patina of Roman coins. They found comparable results to traditional techniques and concluded that gel electrolytes are a good alternative for non-invasive and non-destructive measurements on archaeological metal samples.

Babutzka et al. [25] utilized pure agar with a chloride concentration of 260 ppm on pure zinc with electrochemical frequency modulation (EFM). They found that the gel electrolyte influences the corrosion layer much less than conventional aqueous electrolytes. The study focused on the applicability of EFM for corrosion investigations on zinc as a minimally invasive method. However, the use of EFM is not straight forward and cannot be adapted to different surfaces and metals without further knowledge [25].

Langklotz et al. [19] on the other hand employed pure agar with a chloride concentration of 60 ppm on titanium zinc to study mainly artificial corrosion product layers. They combined the gel electrolyte with ex-situ Fourier-transform infrared spectroscopy (FTIR) and were able to characterize extremely thin zinc surface layers. Measurements with gel electrolytes showed slight changes in the electrochemical behaviour of the zinc layers, which were not yet visible in the FTIR spectra due to very thin layers.

Both authors, Babutzka and Langklotz et al., used the polarization resistance as an indicator for the protectiveness of the corrosion layer. In 2009, Cano et al. [43] reviewed the use of the polarization resistance to examine the protective patina on cultural heritage. In case of uniform corrosion, the polarization resistance provides information about the corrosion rate of samples in a shorter time period than atmospheric exposure tests. The polarization resistance (R_p) can be calculated by different methods, i.e. by EFM, dynamic polarisation [25], linear sweep voltammetry, linear polarisation resistance measurements [19] or by electrochemical impedance spectroscopy [43]. It is important to note, however, that R_p resembles only the polarization resistance for active corroding systems. For all others systems forming protective layers, such as zinc, R_p combines the resistance of the corrosion product, the electrolyte and the charge transfer [19]. Nonetheless, this combination of resistances forms an effective indicator of the protectiveness of the corrosion product layer and, to avoid further confusion, will be called R_L. R_L is defined as corrosion product layer resistance in this paper.

This work aims to implement a serial measurement of the corrosion product layer resistance for the use of zinc and zinc coatings for corrosion monitoring. Unlike the cited authors, the gel pad is not meant to mimic an aqueous electrolyte or to trigger corrosion reactions, but to describe the actual state of the surface layer consisting of corrosion products from exposure in a minimally invasive way. Thus, highly pure agar with a native chloride concentration of 16 mg/ 100 ml dissolved in demineralized water is employed as an electrolyte.

This work is composed of four parts: first, the gel electrolyte made of agar is verified as a method for zinc and zinc-coated samples. In the following part, the corrosion product layer resistance R_L is introduced, which is developed into a serial measurement in part three. Finally, the serial measurement is applied on a representative zinc coating, demonstrating its suitability for practical applications.

Table 2
Ingredients of the high purity agar powder per 100 ml demineralized water.

Chemical compound	Cl^-	PO_4^{3-}	SO_4^{2-}	NO_3^-
Weight	16 mg	7 mg	3 mg	below detection limit

2. Materials & methods

2.1. Electrolyte

All measurements were performed with a gel electrolyte made of high-purity agar (Merck KGaA). The ingredients of the used agar powder per 100 ml demineralized water are displayed in Table 2.

Using an agar concentration of 3% (w/v), 1.5 g agar powder was dissolved in 50 ml demineralized water and boiled under constant stirring at around 90°C. After cooling to 80°C, the liquid agar was poured into a petri dish, leading to a pad thickness of around 2.8 mm. Following solidification, circular gel pads with a diameter of 19 mm were cut out. The resulting measurement area comprised 2.84 cm^2.

2.2. Samples and sample preparation

Zinc with 99.95% purity and electrolytically galvanized steel (Salzgitter Mannesmann Forschung GmbH, Salzgitter, Germany) were used in this work. Both types of working electrodes were supplied with a corrosion protection oil on top of the surface. Hence, the samples were degreased with petroleum ether and subsequently cleaned with ethanol. The cleaning step was performed immediately before the measurements or exposure test.

In this work, pure zinc and electrolytically galvanized samples were used with following surface modifications:

- as-received with cleaned surface as described above; exhibits a thin, undefined layer of ZnO and $Zn(OH)_2$, which cannot be detected with FTIR
- as-received with cleaned surface and exposed to urban atmosphere

Furthermore, some of the pure zinc samples were pickled with the following method:

- pickled with 1 M NaOH

The exposure was performed under urban atmosphere at the headquarter of the Federal Institute for Materials Research and Testing in Berlin-Steglitz. The sample rack is situated on the roof of the main building, 17 m high in relation to the street level. The distance (beeline) to the highly frequented main road B1 is 25 m. The corrosivity category of this atmosphere was determined as C3 (5.3 g/m^2 a) for zinc under free exposure. The exposure test of the pure zinc samples was started on 13 January 2020 and finished 28 days later on 10 February 2020, while the exposure experiment for the electrolytically galvanized samples began on 5 February 2020 and terminated 28 days later on 4 March 2020. Hourly precipitation values were taken from the archive (Climate Data Centre) of Deutscher Wetterdienst [44].

2.3. Electrochemical set-up

The electrochemical experiments were carried out with a Potentiostat/Galvanostat Interface 1000 (Gamry Instruments) and a three-electrode set-up, comprising a counter electrode (CE), a working electrode (WE) and a reference electrode (RE). While a saturated silver/silver chloride electrode (+197 mV vs. SHE) was utilized for the reference electrode, the counter electrode consisted of a titanium-mixed oxide mesh. Zinc or electrolytically galvanized

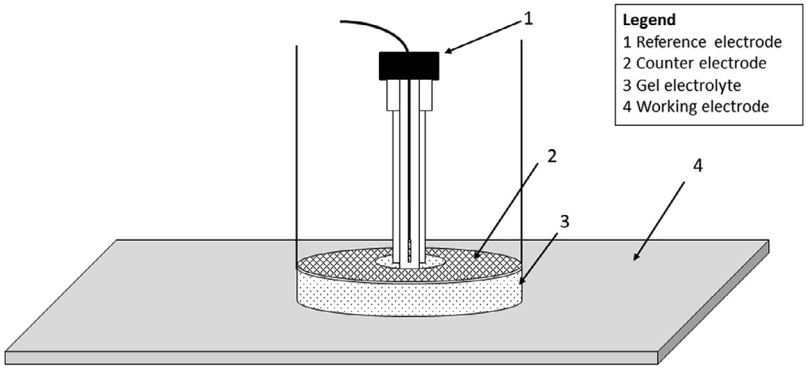

Fig. 1. Scheme of the three-electrode electrochemical set-up used for gel electrolytes (not true to scale).

steel were used as working electrodes. The thickness of the gel pad defined the distance between the reference and the counter electrode to the working electrode. According to Langklotz et al. [19], the influence of the iR-drop inside the gel pad can be neglected.

Fig. 1 displays a schematic drawing of the electrochemical set-up.

2.4. Methods used

Linear polarization was used to determine the corrosion product layer resistance (R_L) of the samples with small deviations of ± 5 mV from the free corrosion potential and a sweep rate dE/dt of 1 mV/s. In this region, the resulting current density (i) -potential (E) plots exhibited an idealized linear behaviour. Eq. (1) determines the corrosion product layer resistance (R_L) based on the i-E plots:

$$R_L = \frac{\Delta E}{\Delta i} \quad (1)$$

All single R_L values were determined after five minutes of open circuit potential measurement, except for the serial R_L measurement where R_L values were recorded every minute beginning from the first contact between sample and gel electrolyte.

Electrochemical impedance spectroscopy was used to characterize the samples after five minutes of measuring the open circuit potential. The selected time of open circuit potential measurement is a compromise between an almost stable potential for further measurements and the targeted minimally invasive measurement of the zinc surfaces. The time of open circuit potential measurement is the shortest possible time that seemed reasonable to prevent changes of the corrosion product layers on the zinc surfaces through an electrolyte.

A sinusoidal electrochemical perturbation of the potential with an amplitude of ± 7.5 mV vs. E_{OCP} was applied in a frequency range of 100 kHz to 0.1 Hz. 10 points per decade were determined. The kinetic values were determined with the help of equivalent circuit models (the models can be seen in the appendix).

The chemical compounds of the surface layers were determined with Fourier-transform infrared spectroscopy (FTIR), using a Nicolet 6700 (Thermo Scientific) with a beam split KBr Mid IR, while a DTGS KBr served as detector. The measurements were assessed between $\nu = 400$ and 4000 cm^{-1} with 32 recordings per measurement.

3. Results & discussion

3.1. Evaluation of the applicability of the gel electrolytes for zinc and zinc coatings

The gel electrolyte method is still comparatively new with regards to the application for zinc and zinc coatings, especially with regards to the composition of the gel. Three successive electrochemical impedance measurements were performed on as-received pure zinc at the same spot to prove that the used gel electrolyte in this work does not influence the measurement itself and the zinc surface. Fig. 2 displays the results. No significant influences are seen between the three measurements, proving that even after the third measurement the result is unchanged compared to the first. Thus, the measurements with agar are minimally invasive and can be used for reactive samples. This is in accordance with results found by other authors [24,25,31].

A clear difference between the long-term exposed and the non-exposed surface states can be seen in Bode and Nyquist plots and the FTIR spectra. A significant difference, however, is not visible among the three measurements on both samples. Thus, the gel electrolyte measurement can give reproducible results.

While in the FTIR spectra no detectable corrosion product layer is visible for the pickled sample and only one small signal for the as-received sample, after the long-term exposure to city atmosphere a typical carbonate-containing corrosion product layer (hydrozincite) appears. This change in the surface state can also be observed in the corresponding Bode plots: the impedance is significantly enhanced due to the growing corrosion product layer, while the phase angle changes from an active to a more diffusion-controlled system. However, the Nyquist plot indicates that a completely diffusion-controlled system is not yet reached. According to the equivalent circuit and the extracted kinetic parameters in Annex B, all three sample states (pickled, as-received and exposed) inherit the same corrosion mechanism. All three samples seem to have a layer of corrosion products on the surface with a porous structure. Nevertheless, the polarization resistance R_P of the exposed samples differs greatly from the other two sample states as it is significantly higher and lies in a different value range.

Subsequently, the reproducibility of results for measuring at different spots needs to be proven. In addition to pure zinc in its as-received state, pickled and weathered samples were investigated. Zinc samples exposed to non-sheltered atmospheric weathering can exhibit different chemical phases on the surface, which do not necessarily cover the surface in a homogeneous way and with different layer thicknesses from the µm to the nm scale [2,19]. Therefore, depending on the sample and the formed corrosion products, the results may differ from pure zinc surfaces as the gel electrolytes are sensitive to different surface states. Fig. 3 shows an example of electrochemical impedance measurements on three different surface states of zinc: a pickled sample, an as-received sample and a sample long-term exposed to urban atmosphere. The fitting of the EIS data to electrical circuits and the extraction of kinetic parameters is performed in Annex B.

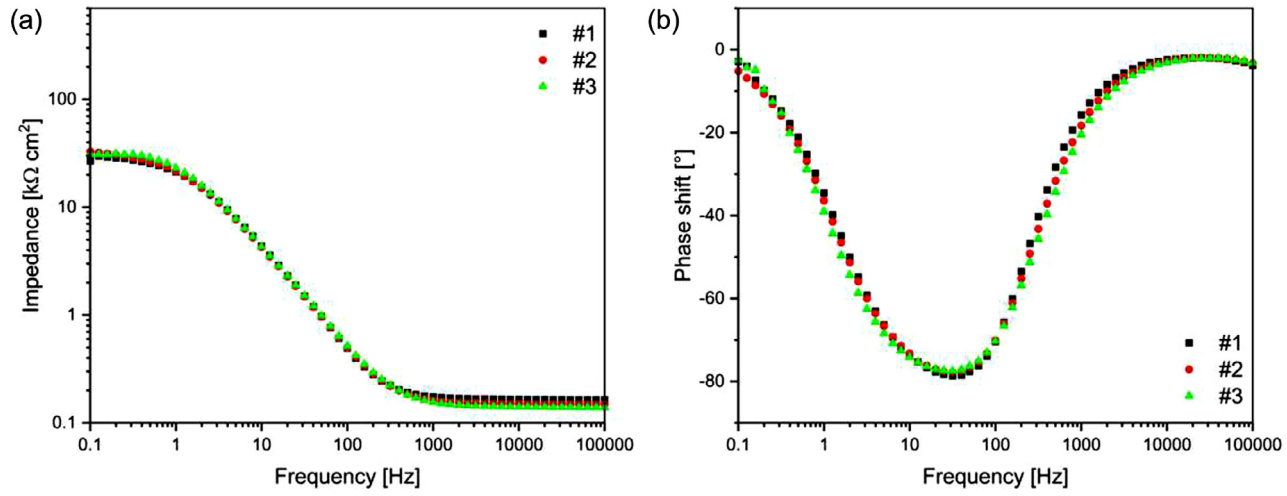

Fig. 2. Successive electrochemical impedance measurements with gel electrolyte on pure zinc showing no influence of the measurement on the results.

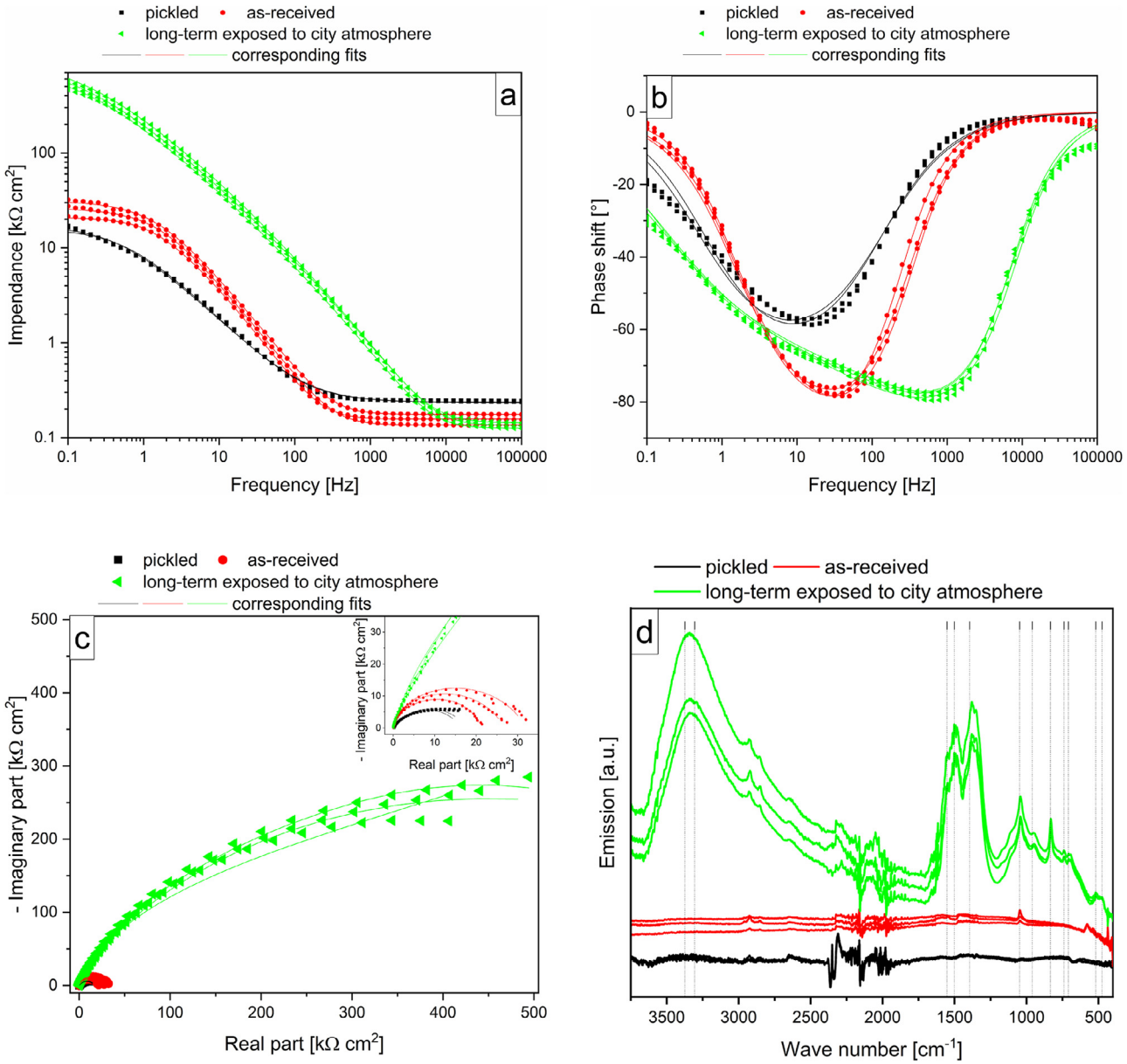

Fig. 3. (a-c) electrochemical impedance measurements: (a) and (b) Bode plots, (c) Nyquist plot with gel electrolyte on zinc samples with three different surface states: pickled, as-received and long-term exposed to urban atmosphere. (d) shows the corresponding FTIR spectra (the marked lines indicate the signals of hydrozincite).

Table 3
Measured and calculated values of R_L from dynamic polarization and R_P from EIS.

Sample state	R_L in kΩ cm^2	R_P in kΩ cm^2
Pickled	16 ± 3	7 ± 1
As-received	22 ± 4	8 ± 3
Long-term exposed	370 ± 35	314 ± 30

The measurements show that the gel electrolyte can detect changes in the chemical composition of the corrosion product layer.

3.2. Introduction of the corrosion product layer resistance R_L and the corresponding serial measurement for enhancing the characterization ability

Various approaches can be chosen to understand the differences between the formed corrosion products mentioned in the previous section: analytical methods such as Fourier-transform infrared spectroscopy (FTIR; as shown in Fig. 3c) or X-Ray diffraction (XRD) need a layer of a minimum thickness, are limited to a specific penetration depth and compounds. Electrochemical impedance measurements need deeper knowledge to be able to interpret the results. On the contrary, the analysis of the corrosion product layer resistance with gel electrolytes is easy to interpret, while it can detect surface changes immediately [19].

The corresponding R_L values of the above example in Fig. 3 are listed in Table 3. In comparison, the polarization resistance of the three states was determined with an equivalent circuit based upon a model including pores (see appendix). The corresponding fits are included in Fig. 3, while the values are added to Table 3. Between the pickled and the as-received sample the difference in resistance is small, as the formed corrosion product layers on the as-received sample is still very thin, instable and inhomogeneous. A significant increase of both resistances is visible upon exposure. Although the trend is similar for both resistances, the measured R_L values are always higher than the calculated polarization resistance values. This is logical, as the R_L value combines different resistances, such as the resistance of the corrosion product, the electrolyte and the charge transfer [19], while the R_P value is only valid for active systems without an oxide layer. However, it can be seen that for an active system (the pickled sample), the R_L is still in the same range of order than the R_P, thus indicating that the tendency of R_L can indeed be used to distinguish between corrosion product layers.

Instead of measuring the corrosion product layer resistance R_L at only one time point after five minutes of OCP, the resistance can also be measured directly after the first contact over an extended time period every minute in a series measurement. Fig. 4 shows exemplary the corrosion product layer resistance and the corresponding potential of the three states pickled, as-received and long-term exposed to city atmosphere. Upon the first contact of sample and gel, a thin moisture film forms at the interface of both. Like the changes occurring at first contact during an open circuit potential measurement, the resistance changes significantly in the first minutes. After this first increase the resistance flattens out for longer measurement times, indicating initial changes in the electrochemical reactions on the surface layer upon exposure and first contact to the electrolyte [24].

The advantage of this series method is that changes on the surface are directly seen, i.e. the wetting process of the surface layer. The serial measurement of R_L after each minute of gel electrolyte contact allows to see immediate changes on the zinc surface and the evaluation of the protective ability. A non-stable corrosion product layer may degrade under the influence of the gel electrolyte but could be determined by a vastly decreasing R_L value during the serial measurement. However, in order to avoid confusion due to a highly complex diagram, for comparing e.g. different exposure times, one should pick one of the time points for all samples to give a clear presentation of the data. A prove that a series measurement does neither influence nor trigger the subsequent measurements can be found in the annex.

3.3. Verification for a representative galvanized coating

In order to verify the serial method and to show that also changes in the R_L value for short-term exposures can be measured, a technically relevant zinc coating, electrolytically galvanized steel sheet, was used in an exposure study (urban atmosphere) over a period of 28 days.

Fig. 5a displays the corrosion product layer resistance during the experiment. Upon the first contact of the samples with the gel electrolyte, the resistance increases, but stabilizes for longer contact times. The as-received sample exhibits a corrosion product layer resistance of around 15 kΩ cm^2. With several precipitation events in the first seven days of exposure time and thus a wet-dry-cycle the corrosion product layer resistance increases significantly to around 50 kΩ cm^2. This indicates the growth of a protective surface layer consisting of corrosion products on the sample surface. With longer exposure times and more precipitation events (Fig. 5f) occurring, the corrosion product layer resistance rises significantly, reaching 180 kΩ cm^2 after 28 days of exposure. This value indicates a stable corrosion product layer [19]. The time needed to form this new layer strongly depends on the atmospheric conditions, such as precipitation and humidity and can therefore not be forecasted.

For a better overview of the corrosion product layer resistances, the values for five minutes contact time of the gel electrolyte are plotted in Fig. 5b. The corrosion product layer resistance increases strongly in the first 14 days, slowing down for longer exposure times, which indicates the transformation of the formed corrosion layer into a stable one. The same trend can be seen for the polarization resistance R_P that was extracted from the EIS measurements by fitting to equivalent circuits. Nevertheless, the R_L value tends to be higher than the R_P value calculated from EIS measurements. It is in accordance to the results in Table 3 on the pure zinc samples.

Fig. 5(c-e) show the bode plot of the phase shift and impedance and the Nyquist plot from EIS of the exposed, electrolytically galvanized samples. The fitting of the EIS data to electrical circuits and the extraction of kinetic parameters is performed in Annex B. The main difference in phase shift occurs between 0 and 7 days of exposure but is still increasing for longer exposure times. The system shifts from a system with a thin and porous corrosion product layer to a more and more diffusion-controlled system that seems to have several differently behaving corrosion product layers on the surface (equivalent circuit in Fig. B.2). The corrosion product layers already formed in the first 7 days, but the increasing phase indicates that the homogeneity of this layer is growing for longer exposure times. The Nyquist plot (e) indicates the intensifying of the diffusion-control by the levelling of the curves.

In contrast, if the FTIR spectra of different exposure times are compared (see Fig. 5e), only slight signals can be seen for 7 days of exposure. The indicated lines mark the signals of hydrozincite ($Zn_5(CO_3)_2(OH)_6$), a carbonate containing layer, which offers a good corrosion protection [19]. The reason for this might be a too thin layer in combination with a rough surface making it not yet detectable by FTIR [19].

While the impedance measurement indicates the main surface change for the first seven days, FTIR shows the first changes for longer times. The measurement of the corrosion product layer resistance (Fig. 5a,b), on the other hand clearly indicates the on-

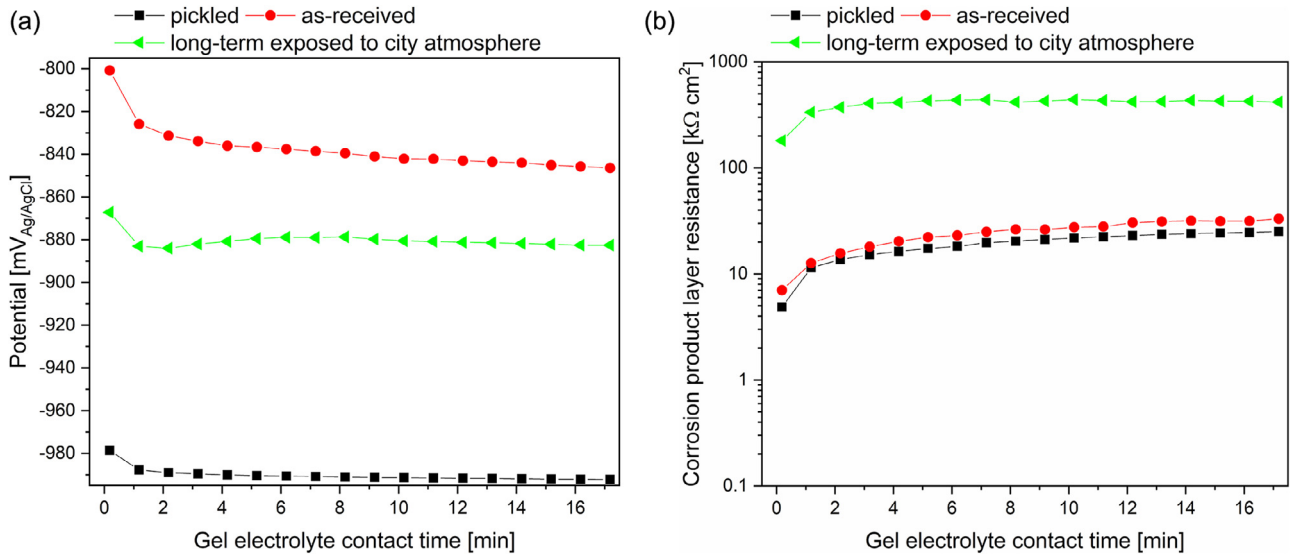

Fig. 4. Series measurement of the corrosion product layer resistance (b) and the corresponding potential (a) of pickled, as-received and long-term exposed zinc over a gel electrolyte contact time of up to 17 min.

going changes on the sample surface upon exposure, both for 7 and up to 28 days of exposure. In contrast to EIS measurements, the corrosion product layer resistance describes this change with a faster and easier to determine measurement. Hence, in this case, the corrosion product layer resistance measurement is superior to the aforementioned methods.

4. Conclusion

The results of this study lead to following conclusions:

1 In contradiction to other studies with gel electrolytes made of agar, in this work the electrolytes were produced for minimally invasive description of the protective power of naturally formed oxide layers. To achieve this, the concentration of ions in the gel electrolyte needs to be as low as possible. Thus, no additions such as salts were used for the gel production.
2 The gel electrolyte does not influence the corrosion product layer of a sample significantly. Hence, it is possible to use gel electrolytes for minimally invasive measurements, which are especially important for soluble and unstable corrosion product layers, which form at the beginning of atmospheric exposure.
3 The measurements with gel electrolytes give highly reproducible results even at different measurement spots.
4 The changes in the phase angle on the EIS bode plots show that the corrosion products constitute a diffusion resistance, which is forming between 0 and 7 days and increases for longer exposure times.
5 The corrosion product layer resistance provides immediate information about slight changes at the sample surface and about the formed corrosion product layer. The results can be verified by electrochemical impedance spectroscopy. FTIR measurements allow verification at longer exposure times.
6 The determination of R_L is a simple and informative method for field measurements. In contrast to electrochemical impedance measurements it is easy to interpret and provides relevant information on the protective ability of a corrosion product layer in a short time.
7 While the polarization resistance R_P cannot be determined on zinc systems with a corrosion product layer, the corrosion product layer resistance R_L can, indicating the current protection ability of the surface or protective layers. The R_L tends to be higher than the R_P value calculated from EIS measurements.

Data availability

The raw/processed data required to reproduce these findings cannot be shared at this time as the data also forms part of an ongoing study.

Declaration of Competing Interest

The authors declare that they have no known competing financial interests or personal relationships that could have appeared to influence the work reported in this paper.

Credit authorship contribution statement

Svenja Valet: Investigation, Methodology, Validation, Writing - original draft. **Andreas Burkert:** Funding acquisition, Project administration, Writing - review & editing. **Gino Ebell:** Writing – review & editing. **Martin Babutzka:** Conceptualization, Funding acquisition, Supervision, Writing - review & editing.

Acknowledgment

This work was supported by the Federal Ministry for Economic Affairs and Energy in the frame of the WIPANO project GELELEK FKZ 03TNH014A.

Annex

A. Influence of the serial measurement

In order to create identical starting conditions, some pure zinc samples were pickled with 1 M NaOH for five minutes ultrasonication, rinsed with ethanol and dried in a warm air flow. The pickling removed the undefined surface layers formed, e.g. zinc oxide and zinc hydroxide. However, pickling of the sample surface cannot be used for field common exposure experiments according to [45–48].

To prove that a series measurement of R_L does neither influence nor trigger the subsequent measurements, the measurement

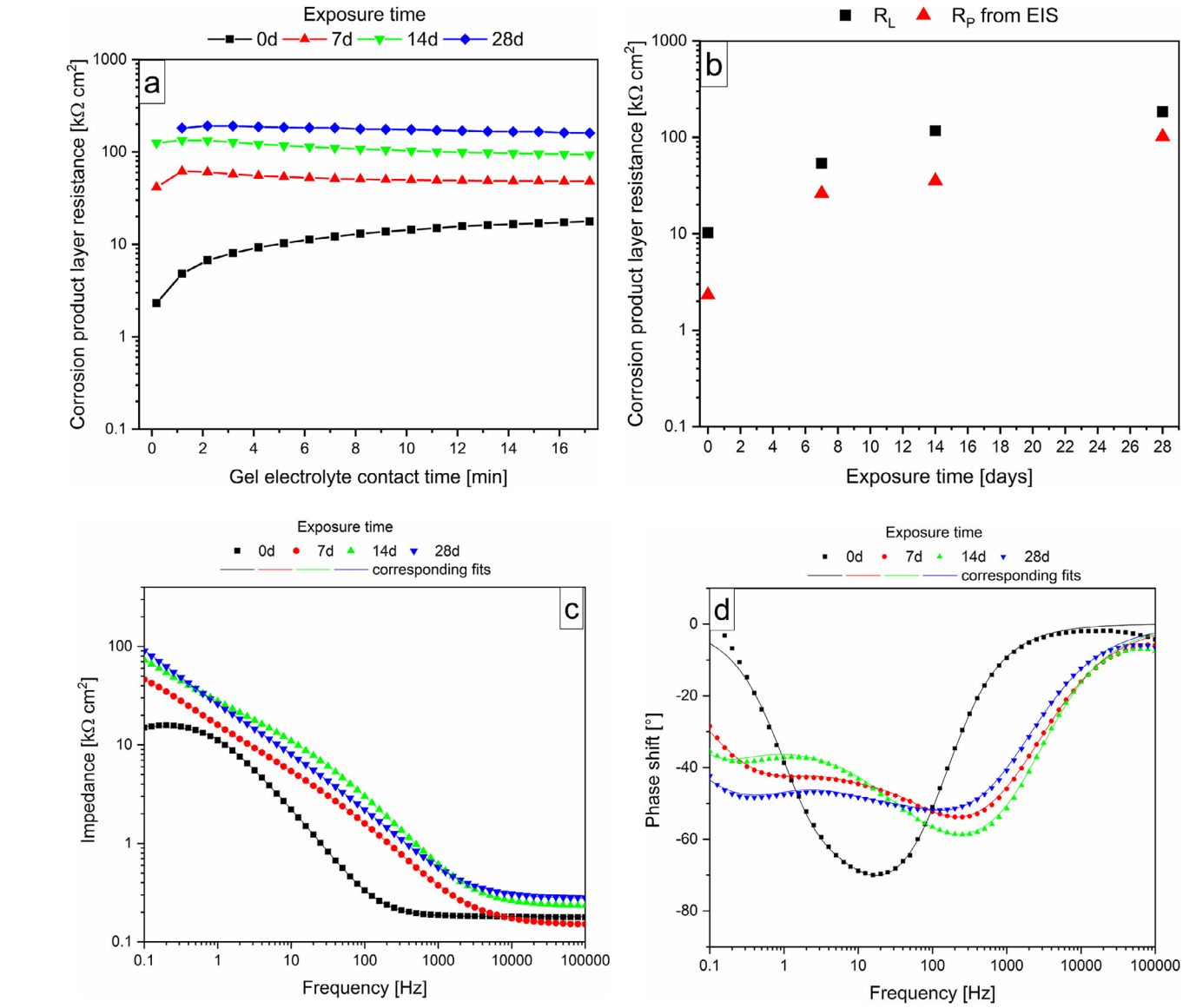

Fig. 5. (a) Serial measurement of the corrosion product layer resistance for the exposure experiment of electrolytically galvanized steel. (b) gives a summary of the serial measurement of the corrosion product layer resistance after five minutes of gel electrolyte contact time and the polarization resistance from EIS measurements according to Tables B.1 and B.2. in the Annex. (c) displays the EIS, bode plot of impedance, (d) phase shift and (e) Nyquist plot. (f) shows the corresponding FTIR measurements (the marked lines indicate the signals of hydrozincite) and (g) the precipitation events; use of gel electrolyte.

series on pickled zinc was started after 0, 5, 10 and 15 min of gel electrolyte contact. Furthermore, single R_L measurements after the same points in time can also be used as a comparison. The resulting values are plotted in Fig. A.1. Significant differences between the results are neither found for the different starting points of the series measurement, nor for single measurements. This clearly indicates that the serial measurement of the corrosion product layer resistance does neither trigger nor influence the measurements or stimulate the results and can be used safely as a method to detect early changes on the surface of zinc substrates.

B. Equivalent circuit and EIS fitting

EIS fitting was carried out with Gamry Echem Analyst Software. The equivalent circuit (Fig. B.1) based upon a model including pores used in Fig. 3 and in Fig. 5 consists of the electrolyte resistance R_{el}, the pore resistance R_{pore} and the polarization resistance R_P, respectively, and two constant phase elements. For the correlation with R_L, only R_P is used. The results of EIS fitting are shown in Table B.1

The equivalent circuit (Fig. B.2) based upon a model including several layers and pores used Fig. 5 consists of the electrolyte resistance R_{el}, two layer resistances $R_{Layer\ 1}$ and $R_{Layer\ 2}$, the polarization resistance R_P, respectively, and three constant phase elements. For the correlation with R_L, only R_P is used. The results of EIS fitting are shown in Table B.2

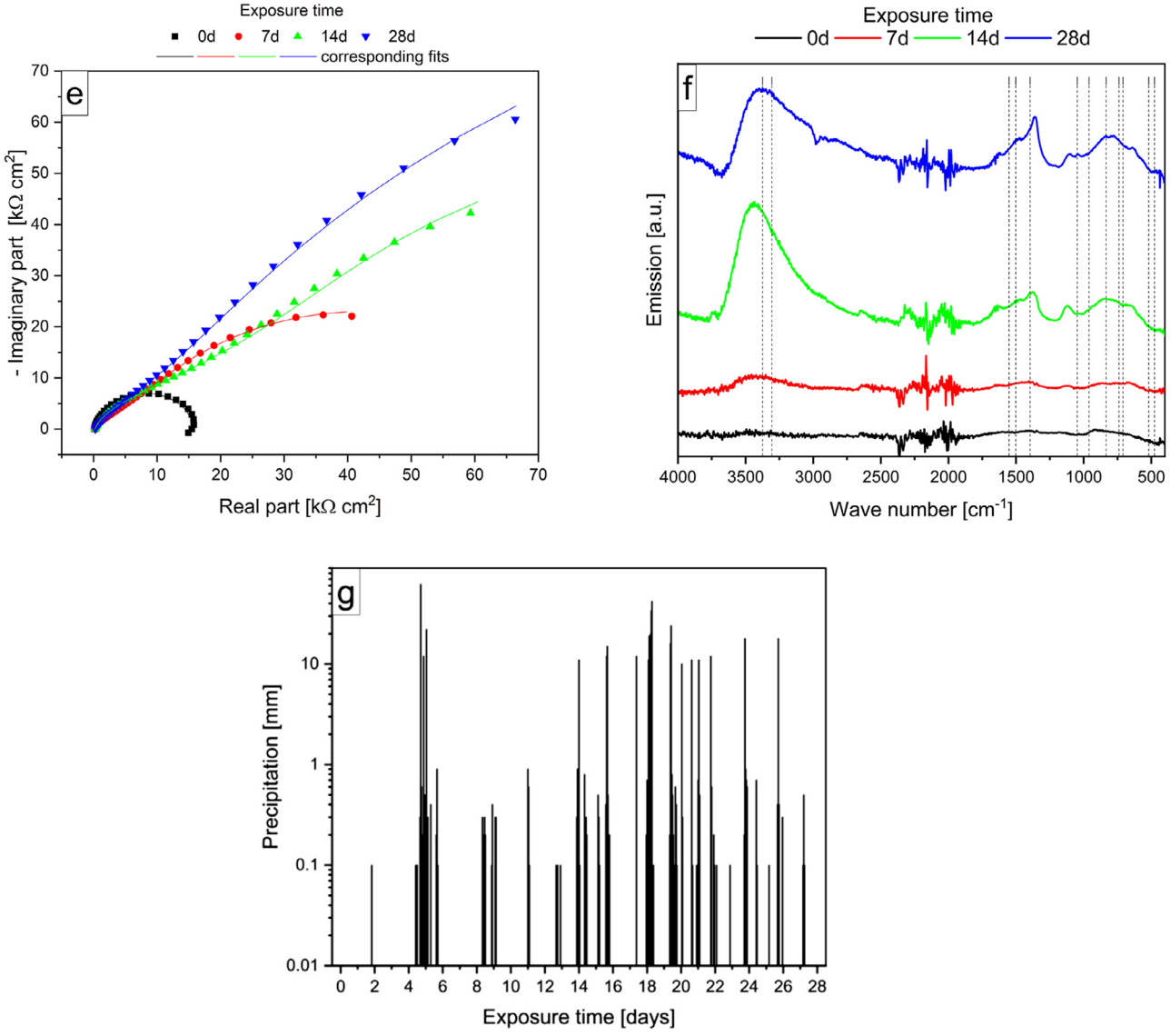

Fig. 5. Continued

Table B.1
Calculated values from fitting of the EIS measurements in Fig. 3 and Fig. 5 to the equivalent circuit in Fig. B.1.

Sample state	R_{el} [Ω]	R_{pore} [kΩ*cm²]	R_P [kΩ*cm²]	Y_{o_pore} [S*s^a]	a_{pore}	Y_{o_CPE} [S*s^a]	a_{CPE}
as-received	48.0	3.8	5.7	$10.2*e^{-6}$	1.0	$32.3*e^{-6}$	0.6
	55.1	0.0	8.4	$12.1*e^{-6}$	1.0	$21.4*e^{-6}$	0.3
	62.1	2.8	8.5	$8.7*e^{-6}$	1.0	$18.8*e^{-6}$	0.6
pickled	86.2	1.0	6.9	$27.7*e^{-6}$	0.9	$103.6*e^{-6}$	0.5
	84.9	0.8	7.5	$31.7*e^{-6}$	0.9	$93.9*e^{-6}$	0.5
long term exposure to city atmosphere	50.2	3.0	328.6	$566.3*e^{-9}$	1.0	$3.5*e^{-6}$	0.6
	47.2	3.6	340.7	$495.6*e^{-9}$	1.0	$3.0*e^{-6}$	0.6
	44.3	2.7	272.3	$574.9*e^{-9}$	1.0	$3.6*e^{-6}$	0.6
Fig. 5 cleaned	63.8	3.2	2.3	$23.37*e^{-6}$	1.0	$22.6*e^{-6}$	1.0

Table B.2
Calculated values from fitting of the EIS measurements in Fig. 5 to the equivalent circuit in Fig. B.2.

Sample state	R_{el} [Ω]	$R_{Layer\ 1}$ [kΩ*cm²]	$R_{Layer\ 2}$ [kΩ*cm²]	$Y_{o\_Layer\ 1}$ [S*s^a]	$a_{Layer\ 1}$	$Y_{o\_Layer\ 2}$ [S*s^a]	$a_{Layer\ 2}$	R_P [kΩ*cm²]	Y_{o_CPE} [S*s^a]	a_{CPE}
exposed 7 d	51.8	1.0	0.8	$13.5*e^{-6}$	0.8	$56.7*e^{-6}$	0.8	26.3	$58.1*e^{-6}$	0.7
exposed 14 d	80.6	2.6	19.5	$4.3*e^{-6}$	0.8	$44.4*e^{-6}$	0.5	35.4	$93.5*e^{-6}$	0.9
exposed 28 d	95.8	1.0	2.0	$10.5*e^{-6}$	0.8	$40.7*e^{-6}$	0.7	102.1	$38.1*e^{-6}$	0.7

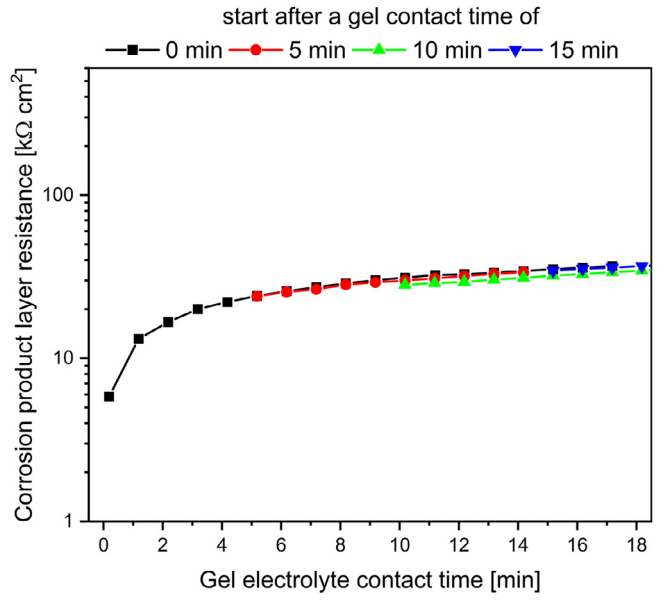

Fig. A.1. Comparison of the serial measurement of R_L with the gel electrolyte on pickled zinc, variation of starting time of the measurement.

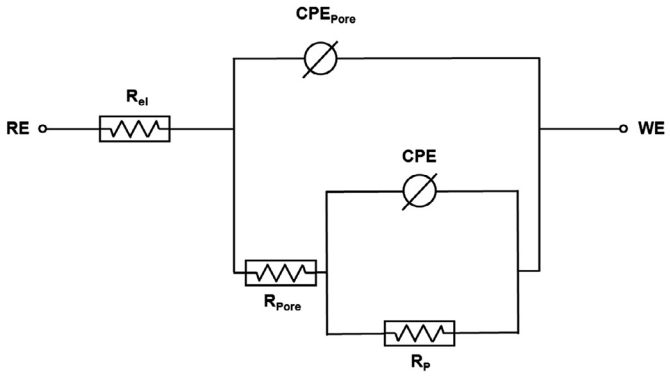

Fig. B.1. Equivalent circuit model including pores.

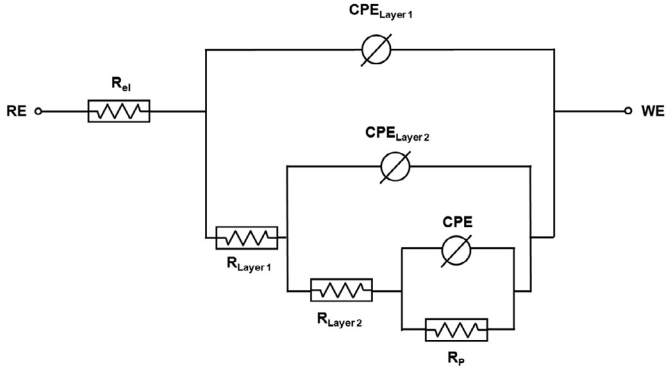

Fig. B.2. Equivalent circuit model including several layers and pores.

References

[1] USGS, *Advance Data Release of the 2017 Annual Tables* 2019, National Minerals Information Center: https://www.usgs.gov/centers/nmic/zinc-statistics-and-information. 2020.

[2] I. Odnevall Wallinder, C. Leygraf, A critical review on corrosion and runoff from zinc and zinc-based alloys in atmospheric environments, Corrosion 73 (9) (2017) 1060–1077.

[3] I. Odnevall, C. Leygraf, Formation of $NaZn_4Cl(OH)_6SO_4$ $6H_2O$ in a marine atmosphere, Corros. Sci. 34 (8) (1993) 1213–1229.

[4] I. Odnevall, C. Leygraf, The formation of $Zn_4Cl_2(OH)_4SO_4$ $5H_2O$ in an urban and an industrial atmosphere, Corros. Sci. 36 (9) (1994) 1551–1559.

[5] I. Odnevall, C. Leygraf, The formation of $Zn_4SO_4(OH)_6 \bullet 4H_2O$ in a rural atmosphere, Corros. Sci. 36 (6) (1994) 1077–1087.

[6] D. Thierry, et al., Atmospheric corrosion of ZnAlMg coated steel during long term atmospheric weathering at different worldwide exposure sites, Corros. Sci. 148 (2018) 338–354.

[7] D. de la Fuente, J.G. Castaño, M. Morcillo, Long-term atmospheric corrosion of zinc, Corros. Sci. 49 (3) (2007) 1420–1436.

[8] M. Fuentes, et al., Atmospheric corrosion of zinc in coastal atmospheres, Mater. Corros. 70 (6) (2019) 1005–1015.

[9] D. Persson, D. Thierry, O. Karlsson, Corrosion and corrosion products of hot dipped galvanized steel during long term atmospheric exposure at different sites world-wide, Corros. Sci. 126 (2017) 152–165.

[10] D. Knotkova, K. Kreislova, S. Dean, ISOCORRAG International Atmospheric Exposure Program: Summary of Results, ASTM International, West Conshohocken, 2010.

[11] E. Almeida, M. Morcillo, B. Rosales, Atmospheric corrosion of zinc Part 1: rural and urban atmospheres, Br. Corros. J. 35 (2000) 284–288.

[12] E. Almeida, M. Morcillo, B. Rosales, Atmospheric corrosion of zinc Part 2: marine atmospheres, Br. Corros. J. 35 (2000) 289–296.

[13] C. Praveen Kumar, et al., Electrodeposition and corrosion behavior of Zn–Ni and Zn–Ni–Fe2O3 coatings, J. Coat. Technol. Res. 9 (2011).

[14] E. Diler, et al., Characterization of corrosion products of Zn and Zn–Mg–Al coated steel in a marine atmosphere, Corros. Sci. 87 (2014) 111–117.

[15] V. Ligier, et al., Formation of the main atmospheric zinc end products: $NaZn_4Cl(OH)_6SO_4$ $6H_2O$, $Zn_4SO_4(OH)_6$ nH_2O and $Zn_4Cl_2(OH)_4SO_4$ $5H_2O$ in $[Cl-]$ $[SO_4^{2-}]$ $[HCO_3-]$ $[H_2O_2]$ electrolytes, Corros. Sci. 41 (6) (1999) 1139–1164.

[16] P. Volovitch, et al., Understanding corrosion via corrosion product characterization: II. Role of alloying elements in improving the corrosion resistance of Zn–Al–Mg coatings on steel, Corros. Sci. 53 (8) (2011) 2437–2445.

[17] T. Prosek, et al., Corrosion performance of Zn–Al–Mg coatings in open and confined zones in conditions simulating automotive applications, Mater. Corros. 61 (5) (2010) 412–420.

[18] N. LeBozec, et al., Corrosion performance of Zn–Mg–Al coated steel in accelerated corrosion tests used in the automotive industry and field exposures, Mater. Corros. 64 (11) (2013) 969–978.

[19] U. Langklotz, et al., The combination of minimally invasive electrochemical investigations and FTIR-spectroscopy to analyze atmospheric corrosion product layers on zinc, Mater. Corros. 70 (2019) 1314–1325.

[20] DINZinc Coatings – Guidelines and Recommendations For the Protection Against Corrosion of Iron and Steel in Structures – Part 1: General principles of Design and Corrosion Resistance (ISO 14713-1:2009); German version EN ISO 14713-1:2009, Beuth Verlag, 2017.

[21] DINCorrosion Tests in Artificial Atmospheres – Salt spray Tests (ISO 9227:2017); German version EN ISO 9227:2017, Beuth Verlag, 2017.

[22] DINHot Dip Galvanized Coatings On Fabricated Iron and Steel Articles – Specifications and Test Methods (ISO 1461:2009); German version EN ISO 1461:2009, Beuth Verlag, 2009.

[23] E.G.G. Association, Salt Spray Testing – Why It Should Not Be Used to Compare Different Types of Coatings, 2013.

[24] G. Monrrabal, et al., Design of gel electrolytes for electrochemical studies on metal surfaces with complex geometry, Electrochim. Acta 220 (2016) 20–28.

[25] M. Babutzka, A. Heyn, Dynamic tafel factor adaption for the evaluation of instantaneous corrosion rates on zinc by using gel-type electrolytes, IOP Conf. Ser. Mater. Sci. Eng. 181 (1) (2017) 012021.

[26] R. Leones, et al., Investigation of polymer electrolyte based on agar and ionic liquids, Express Polym. Lett. 6 (2012) 1007–1016.

[27] V. Di Noto, et al., Polymer electrolytes: present, past and future, Electrochim. Acta 57 (2011) 4–13.

[28] P.V. Wright, Polymer electrolytes-The early days, Electrochim. Acta 43 (10) (1998) 1137–1143.

[29] E. Cano, et al., A novel gel polymer electrolyte cell for *in-situ* application of corrosion electrochemical techniques, Electrochem. Commun. 41 (2014) 16–19.

[30] A.C. Nwanya, et al., Complex impedance and conductivity of agar-based ion-conducting polymer electrolytes, Appl. Phy. A 119 (1) (2015) 387–396.

[31] B. Ramírez Barat, E. Cano, The use of agar gelled electrolyte for in situ electrochemical measurements on metallic cultural heritage, Electrochim. Acta 182 (2015) 751–762.

[32] S. Arnott, et al., The agarose double helix and its function in agarose gel structure, J. Mol. Biol. 90 (2) (1974) 269–284.

[33] M. Lahaye, C. Rochas, Chemical structure and physico-chemical properties of agar, Hydrobiologia 221 (1) (1991) 137–148.

[34] A.J. Spark, et al., Investigation of agar as a soil analogue for corrosion studies, Mater. Corros. 67 (1) (2016) 7–12.

[35] E. Raphael, et al., Agar-based films for application as polymer electrolytes, Electrochim. Acta 55 (4) (2010) 1455–1459.

[36] A. Heyn, Comparison of liquid and gel electrolytes for the investigation of pitting corrosion on stainless steels, IOP Conf. Ser. Mater. Sci. Eng. 882 (2020) 012010.

[37] G. Monrrabal, A. Bautista, F. Velasco, Use of innovative gel electrolytes for electrochemical corrosion measurements on carbon and galvanized steel surfaces, Corrosion 75 (12) (2019) 1502–1512.

[38] E. Angelini, et al., An *in situ* investigation of the corrosion behaviour of a weathering steel work of art, Surf. Interface Anal. 44 (8) (2012) 942–946.

[39] F. Di Turo, et al., A multi-analytical approach for the validation of a jellified electrolyte: application to the study of ancient bronze patina, Microchem. J. 134 (2017) 154–163.
[40] G. Monrrabal, et al., Non-destructive electrochemical testing for stainless-steel components with complex geometry using innovative gel electrolytes, Metals 8 (7) (2018) Basel.
[41] B. Ramírez Barat, E. Cano, P. Letardi, Advances in the design of a gel-cell electrochemical sensor for corrosion measurements on metallic cultural heritage, Sens. Actuators B Chem. 261 (2018) 572–580.
[42] G. Monrrabal, F. Huet, A. Bautista, Electrochemical noise measurements on stainless steel using a gelled electrolyte, Corros. Sci. 148 (2019) 48–56.
[43] E. Cano, D. Lafuente, D.M. Bastidas, Use of EIS for the evaluation of the protective properties of coatings for metallic cultural heritage: a review, J. Solid State Electrochem. 14 (3) (2010) 381–391.
[44] Deutscher Wetterdienst. Climate data center, offenbach Germany. [2020 09.05.2020]; Available from: https://cdc.dwd.de/portal/.
[45] DINCorrosion of Metals and Alloys – Corrosivity of Atmospheres – Classification, Determination and Estimation (ISO 9223:2012); German version EN ISO 9223:2012, Beuth Verlag, 2012.
[46] DINCorrosion of Metals and Alloys – Corrosivity of Atmospheres – Guiding values For the Corrosivity Categories (ISO 9224:2012); German version EN ISO 9224:2012, Beuth Verlag, 2012.
[47] DINCorrosion of Metals and Alloys – Corrosivity of Atmospheres – Measurement of Environmental Parameters Affecting Corrosivity of Atmospheres (ISO 9225:2012); German version EN ISO 9225:2012, Beuth Verlag, 2012.
[48] DINCorrosion of Metals and Alloys – Corrosivity of Atmospheres – Determination of Corrosion Rate of Standard Specimens For the Evaluation of Corrosivity (ISO 9226:2012); German version EN ISO 9226:2012, Beuth Verlag, 2012.